

Millimeter Wave Channel Estimation via Exploiting Joint Sparse and Low-Rank Structures

Xingjian Li, Jun Fang, Hongbin Li, *Senior Member, IEEE*, and Pu Wang

Abstract—We consider the problem of channel estimation for millimeter wave (mmWave) systems, where, to minimize the hardware complexity and power consumption, an analog transmit beamforming and receive combining structure with only one radio frequency (RF) chain at the base station (BS) and mobile station (MS) is employed. Most existing works for mmWave channel estimation exploit sparse scattering characteristics of the channel. In addition to sparsity, mmWave channels may exhibit angular spreads over the angle of arrival (AoA), angle of departure (AoD), and elevation domains. In this paper, we show that angular spreads give rise to a useful low-rank structure that, along with the sparsity, can be simultaneously utilized to reduce the sample complexity, i.e. the number of samples needed to successfully recover the mmWave channel. Specifically, to effectively leverage the joint sparse and low-rank structure, we develop a two-stage compressed sensing method for mmWave channel estimation, where the sparse and low-rank properties are respectively utilized in two consecutive stages, namely, a matrix completion stage and a sparse recovery stage. Our theoretical analysis reveals that the proposed two-stage scheme can achieve a lower sample complexity than a direct compressed sensing method that exploits only the sparse structure of the mmWave channel. Simulation results are provided to corroborate our theoretical results and to show the superiority of the proposed two-stage method.

Index Terms—MmWave channel estimation, angular spread, jointly sparse and low-rank, compressed sensing.

I. INTRODUCTION

Millimeter wave (mmWave) communication is a promising technology for future 5G cellular networks [1]–[3]. It has the potential to offer gigabits-per-second communication data rates by exploiting the large bandwidth available at mmWave frequencies. However, a key challenge for mmWave communication is that signals incur a much more significant path loss over the mmWave frequency bands as compared with the path attenuation over the lower frequency bands [4]. To compensate for the significant path loss, large antenna arrays should be used at both the base station (BS) and the mobile station (MS) to provide sufficient beamforming gain for mmWave communications [5].

Xingjian Li and Jun Fang are with the National Key Laboratory of Science and Technology on Communications, University of Electronic Science and Technology of China, Chengdu 611731, China, Email: JunFang@uestc.edu.cn

Hongbin Li is with the Department of Electrical and Computer Engineering, Stevens Institute of Technology, Hoboken, NJ 07030, USA, E-mail: Hongbin.Li@stevens.edu

Pu Wang is with the Mitsubishi Electric Research Laboratories, Cambridge, MA 02139, USA, E-mail: pwang@merl.com

This work was supported in part by the National Science Foundation of China under Grant 61522104, and the National Science Foundation under Grant ECCS-1408182 and Grant ECCS-1609393.

Although directional beamforming helps overcome the path loss issue, it also complicates the mmWave communication system design. Due to the narrow beam of the antenna array, communication between the transmitter and the receiver is possible only when the transmitter's and receiver's beams are well-aligned, i.e. the beam directions are pointing towards each other. Therefore beamforming training is required to search for the best beamformer-combiner pair that gives the highest channel gain. One method is to exhaustively search for all possible beam pairs to identify the best beam alignment. Nevertheless, this exhaustive search may lead to a prohibitively long training process, particularly when the number of antennas at the BS and MS is large. To address this issue, an adaptive beam alignment algorithm was proposed in [6], where a hierarchical multi-resolution beamforming codebook was employed to avoid the costly exhaustive sampling of all pairs of transmit and receiver beams. Nevertheless, this adaptive beam alignment requires a feedback channel from the receiver to the transmitter, which may not be available before the communication between the receiver and the transmitter is established. Recently, a novel beam steering scheme called as "Agile-Link" [7] was proposed to find the correct beam alignment without scanning the space. The main idea of the Agile-Link is to harness the beam directions using a few carefully chosen hash functions, and steer the antenna array to beam along multiple directions simultaneously.

Unlike beam scanning techniques whose objective is to find the best beam pair, another approach is to directly estimate the mmWave channel or its associated parameters, e.g. angles of arrival/departure, e.g. [8]–[17]. In particular, by exploiting the sparse scattering nature of mmWave channels, mmWave channel estimation can be formulated as a sparse signal recovery problem [10]–[16], and it has been shown that substantial reduction in training overhead can be achieved. Besides the compressed sensing techniques, low-rank tensor factorization methods [17], [18] were recently proposed to exploit the low-rank structure of mmWave channels, and have been shown to outperform the compressed sensing-based methods in terms of both estimation accuracy and computational complexity.

In addition to the sparse scattering characteristic, several real-world measurements in dense-urban propagation environments (e.g. [19]–[22]) reveal that mmWave channels spread in the form of clusters of paths over the angular domains including the angle of arrival (AoA), angle of departure (AoD), and elevation. In [21], [22], real-world channel measurements at 28 and 73 GHz in New York city were reported, in which the angular spread has been explicitly studied in terms of the root mean-squared (rms) beamspread in the different

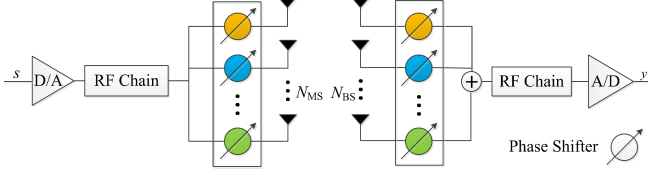


Fig. 1. A block diagram of the analog transmit beamforming and receive combining structure.

angular (AoA, AoD, and elevation) dimensions. Specifically, the measured AoA spreads (in terms of rms) are 15.5° and 15.4° , respectively, for the two carrier frequencies, while the measured AoD spreads (in terms of rms) are 10.2° and 10.5° , respectively. Moreover, the angular spread increases as the spatial resolution becomes finer when the number of antennas at the BS/MS increases. As demonstrated in [23], the angular spreads give rise to a block-sparse structure that can be exploited to improve the mmWave channel estimation performance.

In this paper, we further show that, in the presence of angular spreads, the mmWave channel exhibits a joint sparse and low-rank structure. To better utilize the joint structure, we propose a two-stage compressed sensing scheme, where a low-rank matrix completion stage is first performed and then followed by a compressed sensing stage to recover the mmWave channel. Our analysis reveals that the number of measurements required for exact channel recovery is $\mathcal{O}(pL^2)$ for the proposed two-stage method, where L represents the number of scattering clusters and p is a quantity that measures the maximum angular spread among all scattering clusters. While a direct compressed sensing method that exploits only the sparsity of mmWave channels requires a number of measurements of $\mathcal{O}(p^2L)$. Thus the proposed two-stage compressed sensing method achieves a lower sample complexity than the direct compressed sensing method when $L < p$, which is very likely to hold in dense-urban propagation environments where the angular spreads over the AoA/AoD/elevation domains could be relatively large.

The rest of the paper is organized as follows. The system model and the problem formulation are discussed in Section II. In Section III, we introduce a geometric mmWave channel model with angular spreads and show that the mmWave channel exhibits a joint sparse and low-rank structure. A two-stage compressed sensing method is developed in Section IV, along with a theoretical analysis for the two-stage method. Simulation results are provided in Section V, followed by concluding remarks in Section VI.

II. SYSTEM MODEL AND PRIOR WORK

Consider a point-to-point mmWave MIMO system consisting of N_{BS} antennas at the BS and N_{MS} antennas at the MS. Since the radio frequency (RF) chains are costly and power-consuming at mmWave frequency bands, to minimize the hardware complexity and power consumption, we focus on an analog transmit beamforming and receive combining structure (see Fig. 1) where only one RF chain is employed at the BS and MS. In this structure, transmit beamforming

and receive combining are implemented in the analog domain using digitally controlled phase shifters. At time instant t , the transmitter employs a beamforming vector $\mathbf{f}(t) \in \mathbb{C}^{N_{MS}}$ to transmit a symbol $s(t)$, and at the receiver, the received signals on all antennas are combined with a receive combining vector $\mathbf{z}(t) \in \mathbb{C}^{N_{BS}}$. The combined signal at the receiver can therefore be expressed as

$$y(t) = \mathbf{z}^H(t) \mathbf{H} \mathbf{f}(t) s(t) + w(t) \quad \forall t = 1, \dots, T \quad (1)$$

where $\mathbf{H} \in \mathbb{C}^{N_{BS} \times N_{MS}}$ is the channel matrix, and $w(t)$ denotes the additive Gaussian noise with zero mean and variance σ^2 . Without loss of generality, we set $s(t) = 1$ during the training phase. Note that since the precoder and combiner are implemented by analog phase shifters, entries of $\mathbf{z}(t)$ and $\mathbf{f}(t)$ have constant modulus.

We see that in mmWave systems, the receiver cannot directly observe \mathbf{H} , rather it observes a noisy version of $\mathbf{z}^H \mathbf{H} \mathbf{f}$. This is also referred to as the channel subspace sampling limitation [6], [13], which makes channel estimation a challenging problem. By exploiting the sparse scattering nature of mmWave channels, the channel estimation problem can be formulated as a sparse signal recovery problem (e.g. [6], [13]). Specifically, note that the mmWave channel is usually characterized by a geometric channel model (see, e.g. [11])

$$\mathbf{H} = \sum_{l=1}^L \alpha_l \mathbf{a}_{BS}(\theta_l) \mathbf{a}_{MS}^H(\phi_l) \quad (2)$$

where L is the number of paths, α_l is the complex gain associated with the l th path, $\theta_l \in [0, 2\pi]$ and $\phi_l \in [0, 2\pi]$ are the associated azimuth AoA and azimuth AoD respectively, and $\mathbf{a}_{BS} \in \mathbb{C}^{N_{BS}}$ ($\mathbf{a}_{MS} \in \mathbb{C}^{N_{MS}}$) is the array response vector associated with the BS (MS). Suppose a uniform linear array (ULA) antenna array is used. Then the steering vectors at the BS and the MS can be written as

$$\mathbf{a}_{BS}(\theta_l) = \frac{1}{\sqrt{N_{BS}}} \left[1, e^{j \frac{2\pi}{\lambda} d \sin(\theta_l)}, \dots, e^{j(N_{BS}-1) \frac{2\pi}{\lambda} d \sin(\theta_l)} \right]^T$$

$$\mathbf{a}_{MS}(\phi_l) = \frac{1}{\sqrt{N_{MS}}} \left[1, e^{j \frac{2\pi}{\lambda} d \sin(\phi_l)}, \dots, e^{j(N_{MS}-1) \frac{2\pi}{\lambda} d \sin(\phi_l)} \right]^T$$

where λ is the signal wavelength, and d is the distance between neighboring antenna elements. To formulate the channel estimation as a sparse signal recovery problem, we first express the channel as a beam space MIMO representation as follows

$$\mathbf{H} = \mathbf{A}_{BS} \mathbf{H}_v \mathbf{A}_{MS}^H \quad (3)$$

where $\mathbf{A}_{BS} \triangleq [\mathbf{a}_{BS}(\psi_1), \dots, \mathbf{a}_{BS}(\psi_{N_1})]$ is an overcomplete matrix ($N_1 \geq N_{BS}$) with each column a steering vector parameterized by a pre-discretized AoA, $\mathbf{A}_{MS} \triangleq [\mathbf{a}_{MS}(\omega_1), \dots, \mathbf{a}_{MS}(\omega_{N_2})]$ is an overcomplete matrix (i.e. $N_2 \geq N_{MS}$) with each column a steering vector parameterized by a pre-discretized AoD, and $\mathbf{H}_v \in \mathbb{C}^{N_1 \times N_2}$ is a sparse matrix with L non-zero entries corresponding to the channel path gains $\{\alpha_l\}$. Here the true AoA and AoD parameters are assumed to lie on the discretized grids.

Substituting (3) into (1), we have

$$\begin{aligned} y(t) &= \mathbf{z}^H(t) \mathbf{A}_{\text{BS}} \mathbf{H}_v \mathbf{A}_{\text{MS}}^H \mathbf{f}(t) + w(t) \\ &= \left[(\mathbf{A}_{\text{MS}}^H \mathbf{f}(t))^T \otimes (\mathbf{z}(t)^H \mathbf{A}_{\text{BS}}) \right] \mathbf{h} + w(t) \\ &= (\mathbf{f}(t)^T \otimes \mathbf{z}(t)^H) (\mathbf{A}_{\text{MS}}^* \otimes \mathbf{A}_{\text{BS}}) \mathbf{h} + w(t) \end{aligned} \quad (4)$$

where \otimes denotes the Kronecker product, $()^*$ represents the complex conjugate, and $\mathbf{h} \triangleq \text{vec}(\mathbf{H}_v)$. Collecting all measurements $\{y(t)\}$ and stacking them into a vector $\mathbf{y} \triangleq [y_1 \dots y_T]^T$, we arrive at

$$\begin{aligned} \mathbf{y} &= \begin{bmatrix} (\mathbf{f}(1)^T \otimes \mathbf{z}(1)^H) \\ \vdots \\ (\mathbf{f}(T)^T \otimes \mathbf{z}(T)^H) \end{bmatrix} (\mathbf{A}_{\text{MS}}^* \otimes \mathbf{A}_{\text{BS}}) \mathbf{h} + \mathbf{w} \\ &\triangleq \boldsymbol{\Psi} \mathbf{h} + \mathbf{w} \end{aligned} \quad (5)$$

Estimating \mathbf{h} now can be formulated as a sparse signal recovery problem as follows

$$\begin{aligned} \min \quad & \|\mathbf{h}\|_1 \\ \text{s.t.} \quad & \|\mathbf{y} - \boldsymbol{\Psi} \mathbf{h}\|_2 \leq \varepsilon \end{aligned} \quad (6)$$

where ε is an error tolerance parameter related to noise statistics. Many efficient algorithms such as the fast iterative shrinkage-thresholding algorithm (FISTA) [24] can be employed to solve the above sparse signal recovery problem. Compressed sensing theory tells that, for the noiseless case, we can perfectly recover a high-dimensional sparse signal \mathbf{h} from a much lower dimensional linear measurement vector \mathbf{y} . Thus the compressed sensing-based method has the potential to achieve a substantial training overhead reduction.

III. CHANNEL MODEL WITH ANGULAR SPREADS

In addition to sparsity, mmWave channels may exhibit angular spreads over the AoA, AoD, and elevation domains [21], [22]. The angular spreads are a result of scattering clusters, where each cluster may contribute with multiple rays/paths with closely-spaced AoAs, AoDs and elevations. To more accurately model the angular spread characteristics of mmWave channels, we adopt the following geometric channel model with L clusters

$$\mathbf{H} = \sum_{l=1}^L \left(\sum_{i=1}^I \alpha_{l,i} \mathbf{a}_{\text{BS}}(\theta_l - \vartheta_{l,i}) \right) \left(\sum_{j=1}^J \beta_{l,j} \mathbf{a}_{\text{MS}}^H(\phi_l - \varphi_{l,j}) \right) \quad (7)$$

where each cluster has IJ paths in total, θ_l and ϕ_l represent the mean AoA/AoD associated with each cluster, and $\vartheta_{l,i}$ and $\varphi_{l,j}$ denote the relative AoA and AoD shift from the mean angle. Note that a similar channel model was considered in [25], where each cluster is assumed to contribute multiple rays/paths between the BS and MS. In fact, the above model (7) can be considered as a generalized form of the channel model in [25]. On the other hand, it can be easily observed that the above channel model can also be expressed as a form of (2). Therefore the compressed sensing-based channel estimation scheme (6) still applies. Nevertheless, as to be shown in the following, the mmWave channel with angular spreads not only exhibits sparsity patterns, it also has a meaningful low-rank

structure that can be simultaneously utilized to reduce the sample complexity.

Similar to (3), we express the channel (7) as a beam space MIMO representation

$$\begin{aligned} \mathbf{H} &= \sum_{l=1}^L \mathbf{A}_{\text{BS}} \boldsymbol{\alpha}_l \boldsymbol{\beta}_l^T \mathbf{A}_{\text{MS}}^H = \mathbf{A}_{\text{BS}} \left(\sum_{l=1}^L \boldsymbol{\alpha}_l \boldsymbol{\beta}_l^T \right) \mathbf{A}_{\text{MS}}^H \\ &\triangleq \mathbf{A}_{\text{BS}} \mathbf{H}_v \mathbf{A}_{\text{MS}}^H \end{aligned} \quad (8)$$

where $\boldsymbol{\alpha}_l \in \mathbb{C}^{N_1}$ and $\boldsymbol{\beta}_l \in \mathbb{C}^{N_2}$ represent the virtual representation over the AoA and AoD domain, respectively. Since the angular spread occupies only a small portion of the whole angular domain, both $\boldsymbol{\alpha}_l$ and $\boldsymbol{\beta}_l$ are sparse vectors with only a few nonzero entries concentrated around the mean AoA and AoD associated with the l th cluster. Hence the virtual beam space channel \mathbf{H}_v is a sum of L sparse matrices. Suppose any sparse vector in $\{\boldsymbol{\alpha}_l, \boldsymbol{\beta}_l\}_l$ contains at most p nonzero entries. As a result, \mathbf{H}_v is a sparse matrix with at most $p^2 L$ nonzero entries. Also, \mathbf{H}_v has at most pL nonzero columns and at most pL nonzero rows. Note that due to the limited scattering nature and small angular spreads, we usually have $pL \ll \min\{N_1, N_2\}$. Meanwhile, \mathbf{H}_v has a low rank structure with $\text{rank}(\mathbf{H}_v) = L$. Thus the virtual beam space channel has a simultaneously sparse and low-rank structure.

Our objective is to estimate/recover the joint sparse and low-rank virtual channel \mathbf{H}_v using as few measurements as possible. Estimation of low-rank matrices or sparse matrices from compressed linear measurements has been studied extensively in various settings, e.g. [26]–[30]. However, there is much less research for cases where the matrix of interest is characterized by two structures simultaneously. In particular, how to simultaneously exploit both structures to improve the sample complexity is of most concern. In [31], an efficient two-stage scheme was developed for recovering a sparse, rank-one and positive semi-definite matrix in the context of compressive phase retrieval, and it was shown that the proposed two-stage scheme can achieve a near-optimal sample complexity and enjoys nice robustness guarantees. In the following section, the two-stage scheme is extended to a more general scenario where the mmWave channel to be estimated is not necessarily a rank-one positive semi-definite matrix. We show that an reduced sample complexity can be obtained as compared with simply exploiting the sparsity of the mmWave channel.

IV. TWO-STAGE COMPRESSED SENSING SCHEME

Before proceeding, we revisit the measurement collection model (1) and reformulate this measurement process as a low-rank matrix sampling process. Assume $\mathbf{z}(t)$ and $\mathbf{f}(t)$ are randomly chosen from pre-determined beamforming/combining codebooks \mathcal{Z} and \mathcal{F} , respectively, where the cardinality of the two sets are $|\mathcal{Z}| = N_Z$ and $|\mathcal{F}| = N_F$ and no beam pair $\{\mathbf{z}(t), \mathbf{f}(t)\}$ is reused during the sampling process. Let $\mathbf{Z} \in \mathbb{C}^{N_{\text{BS}} \times N_Z}$ and $\mathbf{F} \in \mathbb{C}^{N_{\text{MS}} \times N_F}$ be matrices constructed by all vectors in \mathcal{Z} and \mathcal{F} , respectively. Then the observation model (1) can be expressed as sampling from a low-rank matrix:

$$\mathbf{Y}_{ij} = (\mathbf{Z}^H \mathbf{H} \mathbf{F})_{ij} \quad (i, j) \in \Omega \quad (9)$$

where $\mathbf{Y} \triangleq \mathbf{Z}^H \mathbf{H} \mathbf{F}$ is a low rank matrix with $\text{rank}(\mathbf{Y}) = L$, \mathbf{Y}_{ij} denotes the (i, j) th entry of \mathbf{Y} , and Ω denotes a set indicating which entries of \mathbf{Y} are observed. We have $|\Omega| = T$. Also, here the observation noise is temporarily ignored to simplify our subsequent analysis.

Suppose \mathbf{Z} and \mathbf{F} are full-rank square matrices, i.e. $N_Z = N_{BS}$ and $N_F = N_{MS}$. Then the problem of estimating \mathbf{H} is equivalent to a low-rank matrix completion problem. Specifically, we first recover the low-rank matrix \mathbf{Y} via a nuclear-norm minimization [28]:

$$\begin{aligned} \min_{\hat{\mathbf{Y}}} \quad & \|\hat{\mathbf{Y}}\|_* \\ \text{s.t.} \quad & \hat{\mathbf{Y}}_{ij} = \mathbf{Y}_{ij} \quad \forall (i, j) \in \Omega \end{aligned} \quad (10)$$

After recovering \mathbf{Y} , the channel \mathbf{H} can be estimated as

$$\hat{\mathbf{H}} = (\mathbf{Z}^H)^{-1} \hat{\mathbf{Y}} \mathbf{F}^{-1} \quad (11)$$

Nevertheless, according to the matrix completion theory [28], the number of measurements has to satisfy

$$T \geq C n^{5/4} L \log(n) \quad (12)$$

in order to stably reconstruct \mathbf{Y} of rank at most L with probability at least $1 - cn^{-3}$, where $n = \max\{N_{BS}, N_{MS}\}$, and the constants $C, c > 0$ are universal. Hence for the low-rank matrix completion approach, the required number of measurements is of order $\mathcal{O}(L \max\{N_{BS}, N_{MS}\}^{5/4})$, which increases approximately linearly with the number of antennas employed at the BS or MS, whichever is greater. We see that the low-rank matrix completion scheme ignores the sparse structure inherent in mmWave channels, and thus can only achieve a sub-optimal sample complexity. To obtain a lower sample complexity, we introduce the following two-stage compressed sensing scheme.

A. Proposed Scheme

The idea of the proposed two-stage scheme is to exploit the low rank and sparse structures in two separate stages. In the first stage, we utilize the low rank structure to recover \mathbf{Y} from observations $\{\mathbf{Y}_{i,j}, (i, j) \in \Omega\}$. Note that \mathbf{Z} and \mathbf{F} do not need to be full-rank; instead, in order to achieve a lower sample complexity, they should have reduced dimensions, i.e. $N_Z < N_{BS}$ and $N_F < N_{MS}$. In other words, the size of \mathbf{Y} is much smaller than the size of \mathbf{H} . In the second stage, based on the reconstructed \mathbf{Y} , we estimate the virtual beam space channel \mathbf{H}_v by exploiting the sparse structure of \mathbf{H}_v . Through this two-stage scheme, the low-rank and sparse structures of the channel matrix \mathbf{H}_v can be effectively decoupled and thus better utilized. For clarity, we summarize the two-stage scheme in Algorithm 1.

B. Theoretical Results

We now provide theoretical guarantees for our proposed two-stage compressed sensing scheme. Our main results are summarized as follows.

Theorem 1: Consider the channel estimation problem described in (9), where the indexes in Ω are uniformly chosen at random with $|\Omega| = T$. The channel matrix \mathbf{H} can be represented in a form of (8). Let L denote the rank of \mathbf{H} , and p

Algorithm 1 Two-Stage Compressed Sensing Algorithm

Given the measurements \mathbf{Y}_Ω , and the matrices $\mathbf{A} \triangleq \mathbf{Z}^H \mathbf{A}_{BS}$, $\mathbf{B} \triangleq \mathbf{A}_{MS}^H \mathbf{F}$.

1 Recover $\hat{\mathbf{Y}}$ by solving

$$\begin{aligned} \min_{\hat{\mathbf{Y}}} \quad & \|\hat{\mathbf{Y}}\|_* \\ \text{s.t.} \quad & \hat{\mathbf{Y}}_{ij} = \mathbf{Y}_{ij} \quad \forall (i, j) \in \Omega \end{aligned} \quad (13)$$

2 Estimate $\hat{\mathbf{H}}_v$ via

$$\begin{aligned} \min_{\hat{\mathbf{H}}_v} \quad & \|\hat{\mathbf{H}}_v\|_1 \\ \text{s.t.} \quad & \hat{\mathbf{Y}} = \mathbf{A}^H \hat{\mathbf{H}}_v \mathbf{B} \end{aligned} \quad (14)$$

denote the maximum number of nonzero entries in $\{\alpha_l, \beta_l\}_l$. Suppose $\mathbf{A} \in \mathbb{C}^{N_Z \times N_1}$ and $\mathbf{B} \in \mathbb{C}^{N_F \times N_2}$ are random matrices with i.i.d. Gaussian random entries $a_{i,j} \sim \mathcal{N}(0, \frac{1}{N_Z})$ and $b_{i,j} \sim \mathcal{N}(0, \frac{1}{N_F})^1$. Define $n \triangleq \max\{N_F, N_Z\}$. There exist positive absolute constants c_1, c_2, c_3, c_4, c_5 and c_6 such that if

$$N_Z \geq c_1 p L \log(N_{BS}/pL) \quad (15)$$

$$N_F \geq c_2 p L \log(N_{MS}/pL) \quad (16)$$

$$T \geq c_3 n^{5/4} L \log(n) \quad (17)$$

then the channel \mathbf{H} can be perfectly recovered from Algorithm 1 with probability exceeding $(1 - c_4 n^{-3})(1 - 2e^{-c_5 N_Z})(1 - 2e^{-c_6 N_F})$.

Proof: Our proof proceeds in two steps. We first investigate the condition under which \mathbf{Y} can be perfectly recovered from (13), and then examine the exact recovery condition for (14). By combining the results of the two stages, we arrive at results in Theorem 1.

Since \mathbf{Y} has a low rank structure, the first stage is essentially a matrix completion stage. Invoking the matrix completion theory [28], we know that for some positive constants c_3 and c_4 , if (17) holds, then \mathbf{Y} can be perfectly recovered with probability exceeding $1 - c_4 n^{-3}$.

The second stage is a sparse matrix recovery stage. Note that \mathbf{H}_v is a sparse matrix with at most pL nonzero columns and rows. We have the following theoretical guarantee for recovering a sparse matrix \mathbf{X} from compressed linear measurements $\mathbf{G} = \mathbf{A} \mathbf{X} \mathbf{B}$.

Lemma 1: Let $\mathbf{X} \in \mathbb{C}^{N_1 \times N_2}$ denote a sparse matrix with at most k nonzero columns and rows. $\mathbf{A} \in \mathbb{C}^{N_A \times N_1}$ and $\mathbf{B} \in \mathbb{C}^{N_B \times N_2}$ satisfy the $2k$ -restricted isometry property with δ_{2k} , namely,

$$\begin{aligned} (1 - \delta_{2k}) \|\mathbf{x}\|_2^2 &\leq \|\mathbf{A} \mathbf{x}\|_2^2 \leq (1 + \delta_{2k}) \|\mathbf{x}\|_2^2 \\ (1 - \delta_{2k}) \|\mathbf{x}\|_2^2 &\leq \|\mathbf{B} \mathbf{x}\|_2^2 \leq (1 + \delta_{2k}) \|\mathbf{x}\|_2^2 \end{aligned}$$

for all $2k$ -sparse vectors \mathbf{x} , where $\delta_{2k} \triangleq \max\{\delta_{2k}(\mathbf{A}), \delta_{2k}(\mathbf{B})\}$, with $\delta_{2k}(\mathbf{A})$ and $\delta_{2k}(\mathbf{B})$ denoting the restricted isometry constants (RIC) of \mathbf{A} and \mathbf{B} respectively.

¹See discussions in Section IV.C regarding this assumption.

If the following condition holds

$$\delta_{2k} < 1 + \sqrt{2} \left(1 - \sqrt{1 + \sqrt{2}} \right) \approx 0.216 \quad (18)$$

then \mathbf{X} can be exactly recovered via

$$\begin{aligned} \min_{\hat{\mathbf{X}}} \quad & \|\hat{\mathbf{X}}\|_1 \\ \text{s.t.} \quad & \mathbf{G} = \mathbf{A}\hat{\mathbf{X}}\mathbf{B}^H \end{aligned} \quad (19)$$

Proof: See Appendix A. \blacksquare

Meanwhile, it is well-known that for a random matrix $\Psi \in \mathbb{R}^{m \times n}$ whose i.i.d. entries follow a Gaussian distribution with zero mean and variance $1/m$, if the following condition

$$m \geq \eta k \log(n/k) \quad (20)$$

holds for a sufficiently large constant $\eta > 0$, then Ψ satisfies the $2k$ -restricted isometry property for a sufficiently small restricted isometry constant $\delta_{2k}(\Psi)$ with probability exceeding $1 - 2e^{-cm}$ for some constant $c > 0$ that depends only on $\delta_{2k}(\Psi)$ [32]. Recalling Lemma 1, we therefore can naturally arrive at the following: for some positive constants c_1, c_2, c_5 and c_6 , if (15) and (16) hold valid, then \mathbf{H}_v can be perfectly recovered via (14) with probability exceeding $(1 - 2e^{-c_5 N_Z})(1 - 2e^{-c_6 N_F})$.

By combining the results from both stages, we now reach that there exist positive absolute constants c_1, c_2, c_3, c_4, c_5 and c_6 such that if (15)–(17) are satisfied, then the channel \mathbf{H} can be perfectly recovered from Algorithm 1 with probability exceeding $(1 - c_4 n^{-3})(1 - 2e^{-c_5 N_Z})(1 - 2e^{-c_6 N_F})$. The proof is completed here. \blacksquare

C. Discussions

From Theorem 1, we see that the number of measurements T required for exact channel recovery is of order

$$\mathcal{O}(p^{5/4} L^{9/4} \log(n)) \approx \mathcal{O}(pL^2) \quad (21)$$

which scales approximately linearly with p and quadratically with the rank L . Since p and L are usually much smaller than $\max\{N_{BS}, N_{MS}\}$, our proposed two-stage scheme can achieve substantial overhead reduction as compared with the low rank matrix completion scheme whose required number of measurements scales linearly with $\max\{N_{BS}, N_{MS}\}$.

It is also interesting to compare our proposed two-stage scheme with a compressed sensing method which solves (9) by directly formulating (9) into a sparse recovery problem (6). Note that $\mathbf{h} = \text{vec}(\mathbf{H}_v)$ has at most $p^2 L$ nonzero entries. According to the compressed sensing theory [26], we know that the probability of successful recovery of \mathbf{h} via (6) exceeds $1 - \delta$ if

$$T \geq Cp^2 L \log(N_1 N_2 / \delta) \quad (22)$$

in which C is a positive constant. Thus the number of measurements required for exact channel recovery is of order

$$\mathcal{O}(p^2 L) \quad (23)$$

for the direct compressed sensing method. Comparing (21) with (23), we can see that our proposed two-stage scheme achieves a lower sample complexity than the direct compressed sensing method if $L < p$. Note that L represents the number of scattering clusters, and p , the largest number of nonzero entries in $\{\alpha_l, \beta_l\}$, is a quantity that measures the maximum angular spread among all scattering clusters. Due to the limited scattering characteristics in mmWave channels, we usually have $L < p$ in practice. In particular, for the extreme case where there is only a line-of-sight (LOS) path between the transmitter and the receiver, L is equal to one, whereas p is generally greater than one since there still exists angular spread (power leakage) due to limited spatial resolution.

In Theorem 1, we assume that $\mathbf{A} \triangleq \mathbf{Z}^H \mathbf{A}_{BS}$ and $\mathbf{B} \triangleq \mathbf{A}_{MS}^H \mathbf{F}$ are random matrices with i.i.d. Gaussian random entries. Nevertheless, noticing that \mathbf{A}_{BS} and \mathbf{A}_{MS} are structured matrices consisting of array response vectors, it may not be possible to devise beamforming and combining matrices $\{\mathbf{Z}, \mathbf{F}\}$ such that the resulting \mathbf{A} and \mathbf{B} satisfy the i.i.d. Gaussian assumption. We, however, still make such an assumption in order to facilitate our theoretical analysis. On the other hand, recent theoretical and empirical studies [33] show that structured matrices also enjoy nice restricted isometry properties. Note that the same problem exists for the direct compressed sensing method, where the sensing matrix is highly structured but a random sensing matrix assumption is evoked in order to obtain its sample complexity.

D. Extension To The Noisy Case

In the previous subsections, we ignore the observation noise in order to simplify our theoretical analysis. Nevertheless, the two-stage compressed sensing scheme can be easily adapted to the noisy case. For clarity, the two-stage algorithm for the noisy case is summarized as follows.

Algorithm 2 Robust Two-Stage Compressed Sensing Algorithm

Given the measurements \mathbf{Y}_Ω , the matrices $\mathbf{A} \triangleq \mathbf{Z}^H \mathbf{A}_{BS}$, $\mathbf{B} \triangleq \mathbf{A}_{MS}^H \mathbf{F}$.

1 Recover $\hat{\mathbf{Y}}$ by solving

$$\begin{aligned} \min \quad & \|\hat{\mathbf{Y}}\|_* \\ \text{s.t.} \quad & \|\hat{\mathbf{Y}}_\Omega - \mathbf{Y}_\Omega\|_F < \varepsilon \end{aligned} \quad (24)$$

2 Estimate $\hat{\mathbf{H}}_v$ via

$$\begin{aligned} \min \quad & \|\mathbf{H}_v\|_1 \\ \text{s.t.} \quad & \|\hat{\mathbf{Y}} - \mathbf{A}^H \mathbf{H}_v \mathbf{B}\|_F < \epsilon \end{aligned} \quad (25)$$

In Algorithm 2, ε and ϵ are error tolerance parameters. Also, the constrained optimizations (24) and (25) can be converted to unconstrained optimization problems by introducing an appropriate choice of the regularization parameter λ . For example, (24) can be replaced by

$$\min_{\hat{\mathbf{Y}}} \quad \|\hat{\mathbf{Y}}_\Omega - \mathbf{Y}_\Omega\|_F^2 + \lambda \|\hat{\mathbf{Y}}\|_* \quad (26)$$

which can be efficiently solved by the fixed point continuation algorithm [34].

V. SIMULATION RESULTS

We now carry out simulation results to illustrate the performance of our proposed two-stage compressed sensing (referred to as two-stage CS) method and its comparison with the direct compressed sensing (referred to as direct-CS) method. For our proposed method, we use the singular value thresholding (SVT) algorithm [35] and the fixed point continuation (FPC) algorithm [34] to solve the matrix completion problem for the noiseless and noisy case, respectively. A fast iterative shrinkage-thresholding algorithm (FISTA) [24] is employed to perform the sparse recovery stage and to solve the direct CS method.

We consider a scenario where both the BS and the MS employ a uniform linear array with $N_{BS} = N_{MS} = 64$ antennas. The distance between neighboring antenna elements is assumed to be half the wavelength of the signal. The mmWave channel is assumed to follow the geometric channel model (7) with $L = 2$ clusters. The mean AoAs/AoDs for these two clusters are set to $\theta_1 = \phi_1 = \pi/6$, $\theta_2 = \phi_2 = -\pi/6$, respectively. The number of rays within each cluster is set to $IJ = 100$. Unless otherwise specified, the AoA and AoD angular spreads for each cluster are set to $\delta_\theta = 15^\circ$ and $\delta_\phi = 10^\circ$. The relative AoA/AoD shifts are uniformly generated within the angular spreads, i.e. $\vartheta_{l,i} \in (\theta_l - \delta_\theta/2, \theta_l + \delta_\theta/2)$, $\varphi_{l,i} \in (\phi_l - \delta_\phi/2, \phi_l + \delta_\phi/2)$. The complex gains $\{\alpha_{l,i}\beta_{l,j}\}$ are assumed to be random variables following a circularly symmetric complex Gaussian distribution $\mathcal{CN}(0, 1/\rho)$, where ρ is given by $\rho = (4\pi D f_c/c)^2$. Here c represents the speed of light, D denotes the distance between the BS and the MS, f_c is the carrier frequency, and we set $D = 30\text{m}$ and $f_c = 28\text{GHz}$. The performance is evaluated via two metrics, namely, the normalized mean squared error (NMSE) and the success rate. The NMSE is calculated as

$$\text{NMSE} = E \left[\frac{\|\hat{\mathbf{H}} - \mathbf{H}\|_F^2}{\|\mathbf{H}\|_F^2} \right] \quad (27)$$

where $\hat{\mathbf{H}}$ denotes the estimate of the true channel \mathbf{H} . The success rate is computed as the ratio of the number of successful trials to the total number of independent runs. A trial is considered successful if the normalized reconstruction error is no greater than 10^{-2} .

In our experiments, the beamforming/combining codebooks, i.e. \mathbf{F} and \mathbf{Z} , are generated according to two different ways. The first is to have the entries of \mathbf{F} and \mathbf{Z} uniformly chosen from a unit circle, in which case the antenna array has a quasi-omnidirectional beam pattern. This scheme is referred to as a random coding (RC) scheme. Another scheme of devising \mathbf{F} and \mathbf{Z} is to steer the antenna array to beam along multiple directions simultaneously, which is achieved by dividing the antenna array into a number of sub-arrays and making each sub-array beam toward an individual direction [7]. The steering directions are randomized for each measurement. This scheme is named as multiple-beam coding (MBC) scheme. In order

to provide a fair comparison, the columns of \mathbf{F} and \mathbf{Z} are normalized to unit norm for both beam pattern design schemes. We assume that, at each time instant, the beamforming vector $\mathbf{f}(t)$ and the combining vector $\mathbf{z}(t)$ are randomly chosen from the beamforming/combining codebooks, respectively. Hence the measurement process can be deemed as randomly collecting samples from a low-rank matrix $\mathbf{Y} = \mathbf{Z}^H \mathbf{H} \mathbf{F}$ (cf. (9)), where \mathbf{Y} is an $N_Z \times N_F$ matrix. For simplicity, we assume $N_Z = N_F$. Also, in our experiments, the value of N_Z (N_F) is adaptively adjusted such that the ratio of the number of observed entries T to the total number of entries in \mathbf{Y} is fixed to be $1/2$, i.e. $T = (1/2)N_Z N_F$. Such a setup can provide a reliable matrix completion result, which in turn helps achieve an accurate channel estimate for our proposed two-stage method. The adaptive adjustment of the dimensions of the codebooks can be easily implemented in practice. We can first generate augmented beamforming/combining codebooks and then choose \mathbf{Z} and \mathbf{F} as subsets (with variable dimensions) of the augmented codebooks.

We now examine the estimation performance of our proposed two-stage CS method and the direct CS method. Fig. 2 plots the success rates for the noiseless case and NMSEs for the noisy case as a function of the number of measurements T , where for the noisy case, the SNR, defined as $10 \log(\|\mathbf{H}\|_F^2 / (N_{BS} N_{MS} \sigma^2))$, is set equal to 20dB. From Fig. 2, we see that better performance can be obtained by using the beamforming/combining codebooks that are generated according to the RC scheme. Also, our proposed two-stage CS method presents a clear performance advantage over the direct CS algorithm, whichever beamforming/combining codebooks are used. This result corroborates our claim that the proposed two-stage CS method can achieve a lower sample complexity than the direct CS method.

Next, in Fig. 3, we examine the performance of respective algorithms as a function of the angular spread, where the AoA and AoD angular spreads are assumed to be the same and vary from 6° to 22° , i.e. $\delta_\theta = \delta_\phi \in [6^\circ, 22^\circ]$. Also, we set $N_Z = N_F = 24$, $T = 0.5N_Z N_F$, and the SNR is set to 20dB for the noisy case. From Fig. 3, we see that the direct CS method outperforms our proposed two-stage scheme when the angular spread is small, say, $\delta_\theta = \delta_\phi = 6^\circ$, whereas our proposed method achieves a performance improvement over the direct CS as the angular spread becomes large. This result, again, substantiates our theoretical analysis. As indicated earlier in our paper, our proposed two-stage scheme achieves a lower sample complexity only when $L < p$, where L represents the number of scattering clusters, and p is a value related to the angular spread. When the angular spread is small, the condition $L < p$ may not hold. As a result, the proposed two-stage CS method does not necessarily perform better than the direct CS method. Lastly, in Fig. 4, we depict the NMSEs of respective algorithms vs. the SNR, where we set $N_Z = N_F = 24$, $T = 0.5N_Z N_F$, $\delta_\theta = 15^\circ$ and $\delta_\phi = 10^\circ$. We see that the proposed two-stage CS method outperforms the direct CS method in moderate and high SNR regimes.

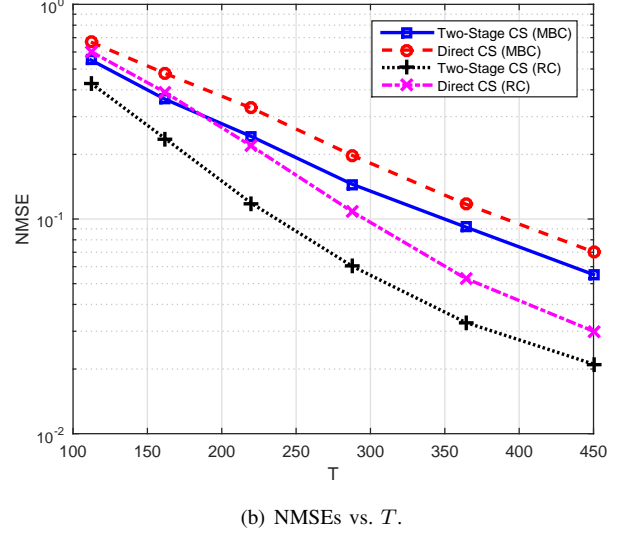
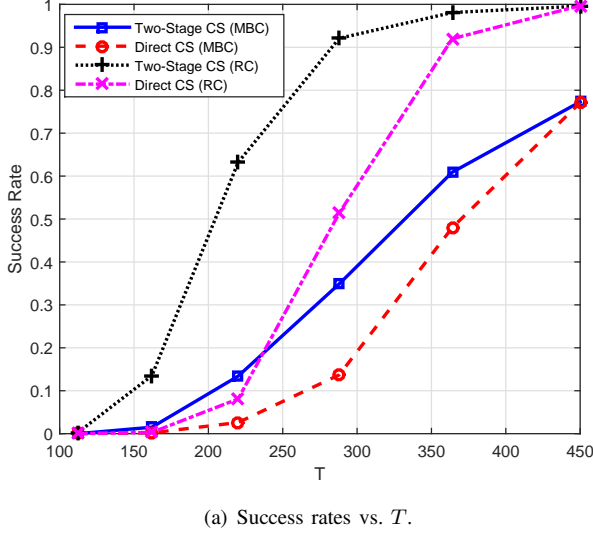


Fig. 2. Success rates and NMSEs of respective algorithms vs. T .

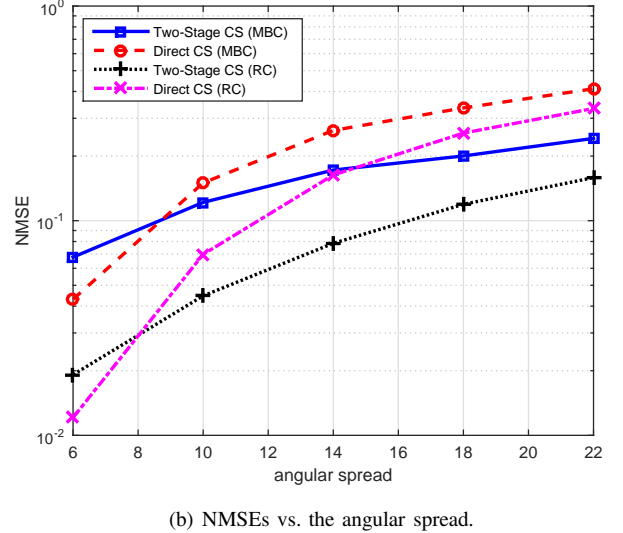
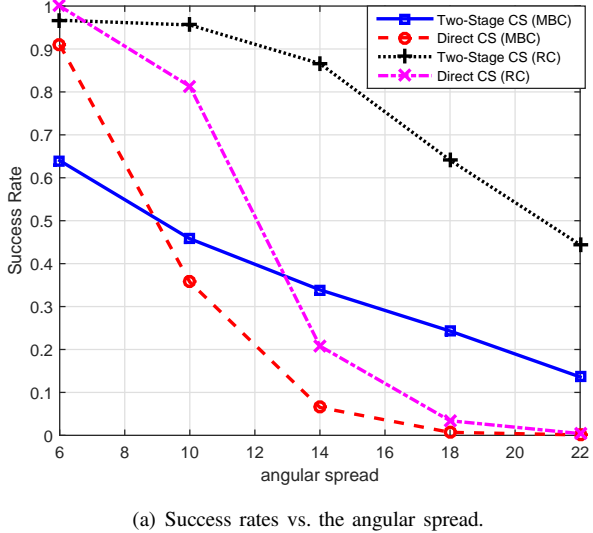


Fig. 3. Success rates and NMSEs of respective algorithms vs. the angular spread.

VI. CONCLUSIONS

We studied the problem of channel estimation for mmWave systems with only one RF chain used at the BS and MS. Besides the sparse scattering characteristics, we also considered the effect of angular spreads in channel modeling and algorithm development. We showed that, in the presence of angular spreads, mmWave channels exhibit a jointly sparse and low-rank structure. A two-stage compressed sensing method was developed, in which a matrix completion stage is first performed, and then followed by a sparse recovery stage to estimate the mmWave channel. Theoretical analysis was also conducted. It reveals that the proposed two-stage method requires fewer measurements than a direct compressed sensing method that exploits the sparsity but ignore the low-rank structure of mmWave channels. Simulation results were pro-

vided to corroborate our theoretical analysis and demonstrate the superiority of the proposed two-stage compressed sensing method.

APPENDIX A PROOF OF LEMMA 1

Before proving $\hat{\mathbf{X}} = \mathbf{X}$, we first show that for any sparse matrix $\Phi \in \mathbb{C}^{N_1 \times N_2}$ with at most $2k$ nonzero columns and rows, we have

$$(1 - \delta_{2k})^2 \|\Phi\|_F^2 \leq \|\mathbf{A}\Phi\mathbf{B}^H\|_F^2 \leq (1 + \delta_{2k})^2 \|\Phi\|_F^2 \quad (28)$$

Since \mathbf{A} satisfies the $2k$ -RIP and each column of Φ is a $2k$ -sparse vector, adding all the inequalities together leads to

$$(1 - \delta_{2k}) \|\Phi\|_F^2 \leq \|\mathbf{A}\Phi\|_F^2 \leq (1 + \delta_{2k}) \|\Phi\|_F^2 \quad (29)$$

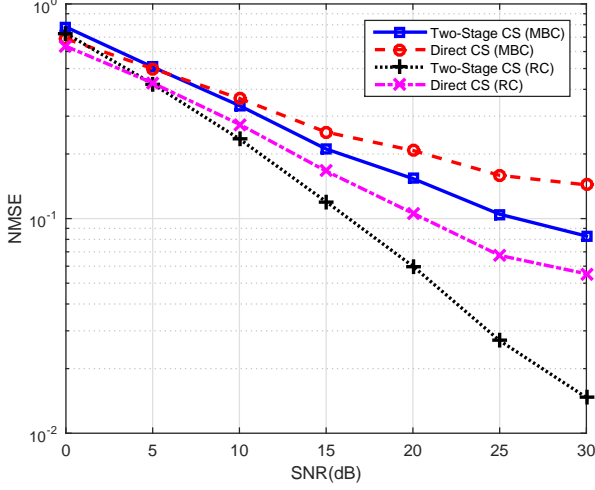


Fig. 4. NMSEs of respective algorithms vs. SNR.

Meanwhile, note that $\Phi^H \mathbf{A}^H$ has at most $2k$ non-zero rows, i.e. each column of $\Phi^H \mathbf{A}^H$ is also a $2k$ -sparse vector. Using the RIP associated with \mathbf{B} , we have

$$\|\mathbf{B}\Phi^H \mathbf{A}^H\|_F^2 \leq (1 + \delta_{2k}) \|\Phi^H \mathbf{A}^H\|_F^2 \leq (1 + \delta_{2k})^2 \|\Phi\|_F^2 \quad (30)$$

$$\|\mathbf{B}\Phi^H \mathbf{A}^H\|_F^2 \geq (1 - \delta_{2k}) \|\Phi^H \mathbf{A}^H\|_F^2 \geq (1 - \delta_{2k})^2 \|\Phi\|_F^2 \quad (31)$$

Combining (30)–(31), we arrive at (28).

Using (28), we now prove that $\mathbf{E} \triangleq \hat{\mathbf{X}} - \mathbf{X}$ equals to zero, i.e. $\|\mathbf{E}\|_F = 0$. Let Ω denotes the support set (i.e. the set of indices of non-zeros entries) of \mathbf{X} . \mathbf{E} can be decomposed as

$$\mathbf{E} = \sum_{i=0}^N \mathbf{E}_i \quad (32)$$

where \mathbf{E}_0 is a matrix whose entries in the set Ω are equivalent to those of \mathbf{E} , while the rest of entries are equal to zero, \mathbf{E}_i ($i \neq 0$) have disjoint support sets with size $k \times k$ such that $(1/k^2)\|\mathbf{E}_i\|_1 \geq \|\mathbf{E}_{i+1}\|_\infty$ for $i = 1, \dots, N-1$. Note that this inequality can be automatically satisfied if we arrange the entries of \mathbf{E} in descending order and ensure that the largest (in terms of magnitude) entry in \mathbf{E}_{i+1} is no greater than the smallest entry in \mathbf{E}_i . Since $\hat{\mathbf{X}}$ is an optimal solution to (19), we have

$$\begin{aligned} \|\mathbf{X}\|_1 &\geq \|\hat{\mathbf{X}}\|_1 = \|\mathbf{E} + \mathbf{X} - \mathbf{E}_0 + \mathbf{E}_0\|_1 \\ &\geq \|\mathbf{E} + \mathbf{X} - \mathbf{E}_0\|_1 - \|\mathbf{E}_0\|_1 \\ &= \|\mathbf{X}\|_1 + \|\mathbf{E} - \mathbf{E}_0\|_1 - \|\mathbf{E}_0\|_1 \end{aligned} \quad (33)$$

Thus we obtain

$$\|\mathbf{E} - \mathbf{E}_0\|_1 \leq \|\mathbf{E}_0\|_1 \stackrel{(a)}{\leq} k\|\mathbf{E}_0\|_F \quad (34)$$

where (a) comes from the Cauchy-Schwarz inequality. Also,

we have

$$\begin{aligned} \|\mathbf{E} - (\mathbf{E}_0 + \mathbf{E}_1)\|_F &= \sum_{i=2}^N \|\mathbf{E}_i\|_F \stackrel{(a)}{\leq} \frac{1}{k} \sum_{i=1}^{N-1} \|\mathbf{E}_i\|_1 \stackrel{(b)}{\leq} \frac{1}{k} \|\mathbf{E}_0\|_1 \\ &\stackrel{(c)}{\leq} \|\mathbf{E}_0\|_F \leq \|\mathbf{E}_0 + \mathbf{E}_1\|_F \end{aligned} \quad (35)$$

where (a) comes from the fact that

$$\|\mathbf{E}_i\|_1 \geq k^2 \|\mathbf{E}_{i+1}\|_\infty \geq k \|\mathbf{E}_{i+1}\|_F \quad (36)$$

and the inequalities (b) and (c) follow from (34). The result (35) implies that

$$\|\mathbf{E}\|_F \leq 2\|\mathbf{E}_0 + \mathbf{E}_1\|_F \quad (37)$$

We now prove $\|\mathbf{E}_0 + \mathbf{E}_1\|_F = 0$. Note that $\mathbf{E}_0 + \mathbf{E}_1$ is a sparse matrix with at most $2k$ nonzero columns and rows.

Using (28), we have

$$\begin{aligned}
(1 - \delta_{2k})^2 \|\mathbf{E}_0 + \mathbf{E}_1\|_F^2 &\leq \left\| \mathbf{A}(\mathbf{E}_0 + \mathbf{E}_1) \mathbf{B}^H \right\|_F^2 \\
&= \text{tr}[(\mathbf{A}(\mathbf{E}_0 + \mathbf{E}_1) \mathbf{B}^H)^H \mathbf{A}(\mathbf{E}_0 + \mathbf{E}_1) \mathbf{B}^H] \\
&= \Re\{\text{tr}[(\mathbf{A}(\mathbf{E}_0 + \mathbf{E}_1) \mathbf{B}^H)^H \mathbf{A} \mathbf{E} \mathbf{B}^H]\} \\
&\quad - \Re\{\text{tr}[(\mathbf{A}(\mathbf{E}_0 + \mathbf{E}_1) \mathbf{B}^H)^H \mathbf{A} \sum_{i=2}^N \mathbf{E}_i \mathbf{B}^H]\} \\
&\leq \Re\{\text{tr}[(\mathbf{A}(\mathbf{E}_0 + \mathbf{E}_1) \mathbf{B}^H)^H \mathbf{A} \mathbf{E} \mathbf{B}^H]\} \\
&\quad + \left| \Re\{\text{tr}[(\mathbf{A}(\mathbf{E}_0 + \mathbf{E}_1) \mathbf{B}^H)^H \mathbf{A} \sum_{i=2}^N \mathbf{E}_i \mathbf{B}^H]\} \right| \\
&\stackrel{(a)}{\leq} \sum_{i=0}^1 \sum_{j=2}^N \left| \Re\{\text{tr}[(\mathbf{A} \mathbf{E}_i \mathbf{B}^H)^H \mathbf{A} \mathbf{E}_j \mathbf{B}^H]\} \right| \\
&= \sum_{i=0}^1 \sum_{j=2}^N \left| \Re\{\text{tr}[(\mathbf{A} \frac{\mathbf{E}_i}{\|\mathbf{E}_i\|_F} \mathbf{B}^H)^H \mathbf{A} \frac{\mathbf{E}_j}{\|\mathbf{E}_j\|_F} \mathbf{B}^H]\} \right| \cdot \|\mathbf{E}_i\|_F \|\mathbf{E}_j\|_F \\
&\stackrel{(b)}{=} \sum_{i=0}^1 \sum_{j=2}^N \frac{1}{4} \left\| \mathbf{A} \left(\frac{\mathbf{E}_i}{\|\mathbf{E}_i\|_F} + \frac{\mathbf{E}_j}{\|\mathbf{E}_j\|_F} \right) \mathbf{B}^H \right\|_F^2 \\
&\quad - \left\| \mathbf{A} \left(\frac{\mathbf{E}_i}{\|\mathbf{E}_i\|_F} - \frac{\mathbf{E}_j}{\|\mathbf{E}_j\|_F} \right) \mathbf{B}^H \right\|_F^2 \cdot \|\mathbf{E}_i\|_F \|\mathbf{E}_j\|_F \\
&\leq \sum_{i=0}^1 \sum_{j=2}^N \frac{1}{4} \left((1 + \delta_{2k})^2 \left\| \frac{\mathbf{E}_i}{\|\mathbf{E}_i\|_F} + \frac{\mathbf{E}_j}{\|\mathbf{E}_j\|_F} \right\|_F^2 \right. \\
&\quad \left. - (1 - \delta_{2k})^2 \left\| \frac{\mathbf{E}_i}{\|\mathbf{E}_i\|_F} - \frac{\mathbf{E}_j}{\|\mathbf{E}_j\|_F} \right\|_F^2 \right) \cdot \|\mathbf{E}_i\|_F \|\mathbf{E}_j\|_F \\
&\stackrel{(c)}{=} \sum_{i=0}^1 \sum_{j=2}^N \frac{1}{4} ((1 + \delta_{2k})^2 \left(\left\| \frac{\mathbf{E}_i}{\|\mathbf{E}_i\|_F} \right\|_F^2 + \left\| \frac{\mathbf{E}_j}{\|\mathbf{E}_j\|_F} \right\|_F^2 \right) \\
&\quad - (1 - \delta_{2k})^2 \left(\left\| \frac{\mathbf{E}_i}{\|\mathbf{E}_i\|_F} \right\|_F^2 + \left\| \frac{\mathbf{E}_j}{\|\mathbf{E}_j\|_F} \right\|_F^2 \right)) \cdot \|\mathbf{E}_i\|_F \|\mathbf{E}_j\|_F \\
&= \sum_{i=0}^1 \sum_{j=2}^N \frac{1}{2} ((1 + \delta_{2k})^2 - (1 - \delta_{2k})^2) \cdot \|\mathbf{E}_i\|_F \|\mathbf{E}_j\|_F \\
&= 2\delta_{2k} \sum_{i=0}^1 \sum_{j=2}^N \|\mathbf{E}_i\|_F \|\mathbf{E}_j\|_F \\
&= 2\delta_{2k} (\|\mathbf{E}_0\|_F + \|\mathbf{E}_1\|_F) \sum_{j=2}^N \|\mathbf{E}_j\|_F \\
&\stackrel{(d)}{\leq} 2\delta_{2k} (\|\mathbf{E}_0\|_F + \|\mathbf{E}_1\|_F) \|\mathbf{E}_0 + \mathbf{E}_1\|_F \\
&\stackrel{(e)}{\leq} 2\sqrt{2}\delta_{2k} \|\mathbf{E}_0 + \mathbf{E}_1\|_F^2 \tag{38}
\end{aligned}$$

where (a) comes from the fact that

$$\mathbf{A} \mathbf{E} \mathbf{B}^H = \mathbf{A} \mathbf{X} \mathbf{B}^H - \mathbf{A} \hat{\mathbf{X}} \mathbf{B}^H = \mathbf{0} \tag{39}$$

(b) follows from the equality

$$4\Re\{\text{tr}(\mathbf{P} \mathbf{Q}^H)\} = \|\mathbf{P} + \mathbf{Q}\|_F^2 - \|\mathbf{P} - \mathbf{Q}\|_F^2 \tag{40}$$

for any complex matrices \mathbf{P} and \mathbf{Q} , (c) is due to the reason that \mathbf{E}_i and \mathbf{E}_j have disjoint supports, (d) follows from (35),

and (e) can be easily verified by noting that

$$\|\mathbf{E}_0 + \mathbf{E}_1\|_F = (\|\mathbf{E}_0\|_F^2 + \|\mathbf{E}_1\|_F^2)^{1/2} \tag{41}$$

If $2\sqrt{2}\delta_{2k} - (1 - \delta_{2k})^2 < 0$, i.e. $\delta_{2k} < 1 + \sqrt{2}(1 - \sqrt{1 + \sqrt{2}})$, then we have $\|\mathbf{E}_0 + \mathbf{E}_1\|_F = 0$ from (38), which implies that $\|\mathbf{E}\|_F = 0$, i.e. $\mathbf{X} = \hat{\mathbf{X}}$. The proof is completed here.

REFERENCES

- [1] T. S. Rappaport, J. N. Murdock, and F. Gutierrez, "State of the art in 60-GHz integrated circuits and systems for wireless communications," *Proc. IEEE*, vol. 99, no. 8, pp. 1390–1436, Aug. 2011.
- [2] S. Rangan, T. S. Rappaport, and E. Erkip, "Millimeter-wave cellular wireless networks: potentials and challenges," *Proc. IEEE*, vol. 102, no. 3, pp. 366–385, March 2014.
- [3] A. Ghosh, T. A. Thomas, M. C. Cudak, R. Ratasuk, P. Moorut, F. W. Vook, T. S. Rappaport, G. R. MacCartney, S. Sun, and S. Nie, "Millimeter-wave enhanced local area systems: a high-data-rate approach for future wireless networks," *IEEE J. Sel. Areas Commun.*, vol. 32, no. 6, pp. 1152–1163, June 2014.
- [4] A. L. Swindlehurst, E. Ayanoglu, P. Heydari, and F. Capolino, "Millimeter-wave massive MIMO: the next wireless revolution?" *IEEE Commun. Mag.*, vol. 52, no. 9, pp. 56–62, September 2014.
- [5] A. Alkhateeb, J. Mo, N. Gonzalez-Prelcic, and R. Heath, "MIMO precoding and combining solutions for millimeter-wave systems," *IEEE Commun. Mag.*, vol. 52, no. 12, pp. 122–131, December 2014.
- [6] S. Hur, T. Kim, D. J. Love, J. V. Krogmeier, T. A. Thomas, and A. Ghosh, "Millimeter wave beamforming for wireless backhaul and access in small cell networks," *IEEE Trans. Commun.*, vol. 61, no. 10, pp. 4391–4403, October 2013.
- [7] O. Abari, H. Hassanieh, M. Rodriguez, and D. Katabi, "Millimeter wave communications: From point-to-point links to agile network connections," in *Proc. 15th ACM Workshop on Hot Topics in Networks*, Atlanta, Georgia, USA, November 9–10 2016, pp. 169–175.
- [8] D. Ramasamy, S. Venkateswaran, and U. Madhow, "Compressive adaptation of large steerable arrays," in *Proc. 2012 Information Theory and Applications Workshop (ITA)*, San Diego, California, USA, February 5–10 2012, pp. 234–239.
- [9] —, "Compressive tracking with 1000-element arrays: A framework for multi-gbps mm wave cellular downlinks," in *Proc. 50th Annual Allerton Conference on Commun., Control, and Comput.*, October 2012, pp. 690–697.
- [10] A. Alkhateeb, G. Leus, and R. Heath, "Compressed sensing based multi-user millimeter wave systems: How many measurements are needed?" in *Proc. 40th IEEE Inter. Conf. on Acoust., Speech and Signal Process. (ICASSP)*, Brisbane, Australia, April 19–24 2015, pp. 2909–2913.
- [11] A. Alkhateeb, O. E. Ayach, G. Leus, and R. Heath, "Channel estimation and hybrid precoding for millimeter wave cellular systems," *IEEE J. Sel. Topics Signal Process.*, vol. 8, no. 5, pp. 831–846, October 2014.
- [12] P. Schniter and A. Sayeed, "Channel estimation and precoder design for millimeter-wave communications: The sparse way," in *Proc. 48th Asilomar Conf. Signals, Syst. Comput.*, Pacific Grove, California, USA, November 2–5 2014, pp. 273–277.
- [13] T. Kim and D. J. Love, "Virtual AoA and AoD estimation for sparse millimeter wave MIMO channels," in *Proc. 16th IEEE Inter. Workshop on Signal Process. Advances in Wireless Commun. (SPAWC)*, Stockholm, Sweden, June 28 – July 1 2015, pp. 146–150.
- [14] Z. Marzi, D. Ramasamy, and U. Madhow, "Compressive channel estimation and tracking for large arrays in mm-Wave picocells," *IEEE J. Sel. Topics Signal Process.*, vol. 10, no. 3, pp. 514–527, April 2016.
- [15] Z. Gao, L. Dai, Z. Wang, and S. Chen, "Spatially common sparsity based adaptive channel estimation and feedback for FDD massive MIMO," *IEEE Trans. Signal Process.*, vol. 63, no. 23, pp. 6169–6183, December 2015.
- [16] X. Gao, L. Dai, and A. M. Sayeed, "Low RF-complexity technologies for 5G millimeter-wave MIMO systems with large antenna arrays," available at [arXiv:1607.04559](https://arxiv.org/abs/1607.04559), 2016.
- [17] Z. Zhou, J. Fang, L. Yang, H. Li, Z. Chen, and S. Li, "Channel estimation for millimeter-wave multiuser MIMO systems via PARAFAC decomposition," *IEEE Trans. Wireless Commun.*, vol. 15, no. 11, pp. 7501–7516, November 2016.

- [18] Z. Zhou, J. Fang, L. Yang, H. Li, Z. Chen, and R. S. Blum, "Low-rank tensor decomposition-aided channel estimation for millimeter wave mimo-ofdm systems," *IEEE Journal Selected Areas in Communications*, to appear.
- [19] M. Samimi, K. Wang, Y. Azar, G. N. Wong, R. Mayzus, H. Zhao, J. K. Schulz, S. Sun, F. Gutierrez, and T. S. Rappaport, "28 GHz angle of arrival and angle of departure analysis for outdoor cellular communications using steerable beam antennas in New York city," in *Proc. 2013 IEEE 77th Vehicular Technology Conference (VTC Spring)*, Dresden, Germany, June 2-5 2013, pp. 1-6.
- [20] H. Zhao, R. Mayzus, S. Sun, M. Samimi, J. K. Schulz, Y. Azar, K. Wang, G. N. Wong, F. Gutierrez, and T. S. Rappaport, "28 GHz millimeter wave cellular communication measurements for reflection and penetration loss in and around buildings in New York city," in *Proc. 2013 IEEE International Conference on Communications (ICC)*, Budapest, Hungary, June 9-13 2013, pp. 5163-5167.
- [21] T. S. Rappaport, S. Sun, R. Mayzus, H. Zhao, Y. Azar, K. Wang, G. N. Wong, J. K. Schulz, M. Samimi, and F. Gutierrez, "Millimeter wave mobile communications for 5G cellular: It will work!" *IEEE Access*, vol. 1, pp. 335-349, May 2013.
- [22] M. R. Akdeniz, Y. Liu, M. K. Samimi, S. Sun, S. Rangan, T. S. Rappaport, and E. Erkip, "Millimeter wave channel modeling and cellular capacity evaluation," *IEEE J. Sel. Areas Commun.*, vol. 32, no. 6, pp. 1164-1179, June 2014.
- [23] P. Wang, M. Pajovic, P. V. Orlik, T. Koike-Akino, K. J. Kim, and J. Fang, "Sparse channel estimation in millimeter wave communications: Exploiting joint AoD-AoA angular spread," in *Proc. 2017 IEEE International Conference on Communications (ICC)*, Paris, France, May 21-25 2017.
- [24] A. Beck and M. Teboulle, "A fast iterative shrinkage-thresholding algorithm for linear inverse problems," *SIAM J. Imaging Sci.*, vol. 2, no. 1, pp. 183-202, March 2009.
- [25] A. Alkhateeb and R. W. Heath, "Frequency selective hybrid precoding for limited feedback millimeter wave systems," *IEEE Trans. Commun.*, vol. 64, no. 5, pp. 1801-1818, May 2016.
- [26] E. Candès and T. Tao, "Decoding by linear programming," *IEEE Trans. Information Theory*, no. 12, pp. 4203-4215, Dec. 2005.
- [27] J. A. Tropp and A. C. Gilbert, "Signal recovery from random measurements via orthogonal matching pursuit," *IEEE Trans. Information Theory*, vol. 53, no. 12, pp. 4655-4666, Dec. 2007.
- [28] E. J. Candès and B. Recht, "Exact matrix completion via convex optimization," *Foundations of Computational Mathematics*, vol. 9, no. 6, pp. 717-772, December 2009.
- [29] B. Recht, M. Fazel, and P. A. Parrilo, "Guaranteed minimum-rank solutions of linear matrix equations via nuclear norm minimization," *SIAM Review*, vol. 52, no. 3, pp. 471-501, August 2010.
- [30] V. Koltchinskii, K. Lounici, and A. B. Tsybakov, "Nuclear-norm penalization and optimal rates for noisy low-rank matrix completion," *The Annals of Statistics*, vol. 39, no. 5, pp. 2302-2329, October 2011.
- [31] S. Bahmani and J. Romberg, "Efficient compressive phase retrieval with constrained sensing vectors," in *Advances in Neural Information Processing Systems (NIPS)*, vol. 28, Montreal, Quebec, Canada, December 7-12 2015, pp. 523-531.
- [32] R. Baraniuk, M. Davenport, R. DeVore, and M. Wakin, "A simple proof of the restricted isometry property for random matrices," *Constructive Approximation*, vol. 28, no. 3, pp. 253-263, January 2008.
- [33] M. F. Duarte and Y. C. Eldar, "Structured compressed sensing: From theory to applications," *IEEE Transactions on Signal Processing*, vol. 59, no. 9, pp. 4053-4085, September 2011.
- [34] S. Ma, D. Goldfarb, and L. Chen, "Fixed point and bregman iterative methods for matrix rank minimization," *Mathematical Programming*, vol. 128, no. 1, pp. 321-353, June 2011.
- [35] J. Cai, E. J. Candès, and Z. Shen, "A singular value thresholding algorithm for matrix completion," *SIAM Journal on Optimization*, vol. 20, no. 4, pp. 1956-1982, March 2010.